COVER SHEET

Title: **Simulation of Arbitrary Delamination Growth in Composite Structures Using the Virtual Crack Extension Method**

Authors: Brett R. Davis
Paul A. Wawrzynek
Anthony R. Ingraffea

ABSTRACT

A finite-element-based toolset has been developed to simulate arbitrary evolution of 3-D, geometrically explicit, interlaminar delaminations in composite structures. A new energy-based growth formulation uses the virtual crack extension (VCE) method to predict point-by-point growth along the delamination front. The VCE method offers an accurate and computationally efficient means to extract both energy release rate, G, and rate of change of energy release rate, $\frac{dG}{da}$, from a single finite element analysis. A new VCE implementation is used to decouple and compute 3-D, mixed-mode, fracture parameters, permitting the use of mixed-mode growth criteria. The $\frac{dG}{da}$ parameters create an influence matrix that relates an extension at one point to the energy release rate elsewhere along the delamination front. The use of the $\frac{dG}{da}$ matrix, in conjunction with an iterative approach that continually updates the delamination configuration by re-meshing, enables the prediction of arbitrary delamination evolution. The numerical techniques and formulations implemented allow a delamination to grow by the rules of mechanics and physics, while reducing computational artifacts, e.g. mesh bias. The evolution of an initial embedded elliptical delamination under central point-loads into a circular configuration is simulated as a proof-of-concept for the new growth formulation.

INTRODUCTION

Laminated, fiber-reinforced, composite materials are used in a variety of applications, including the aerospace and marine industries. Although laminated composite structures have been in use for decades, fully understanding and accurately predicting their failure mechanisms remains a significant challenge. The current work seeks to address this challenge for one of the most common modes of failure: delamination. A variety of finite-element-based approaches has been

Cornell University, School of Civil and Environmental Engineering
638 Frank H.T. Rhodes Hall, Ithaca, NY 14853, U.S.A.

developed to handle the problem of progressive delamination growth. These include damage mechanics [1], cohesive crack models [2], nodal release methods via the virtual crack closure technique (VCCT) [3,4] and the extended finite element method (XFEM) [5]. This paper describes the development of a new approach, one that reduces computational limitations, freeing the mechanics and physics to dictate the evolution of the delamination.

Perhaps the most widely utilized of the aforementioned are cohesive zone models and nodal release methods. However, these methods limit the characterization of delamination growth by constraining the evolution to the geometry of the predetermined finite element mesh. Cohesive zone elements use traction-displacement curves to govern behavior at the delamination front. When the traction-displacement relationship reaches its limit, i.e. maximum displacement, and zero traction, the cohesive element is eliminated, thus extending the delamination. Alternatively, fracture mechanics methods are used to calculate stress intensity factors or energy release rates at the front, and identify nodes to be released to extend the front. In either case, the delamination path will only follow existing element boundaries, restricting the direction and distance of the predicted advance of the front. These growth prediction approaches have the potential to produce saw-tooth, jagged delamination fronts that do not match physical configurations, as seen in Figure 1.

To minimize these limitations, one can use a heavily refined mesh around the front, greatly inflating the computational cost, or one can produce meshes constructed with knowledge of the expected delamination growth pattern. However, this latter technique contradicts the notion of arbitrary evolution by linking a physical feature, delamination shape, with a computational artifact, the mesh. For example, with an initial circular flaw, one might design a mesh that contains an organization of elements in a concentric circular pattern around the initial delamination, Figure 2. However, of interest here is what happens when the

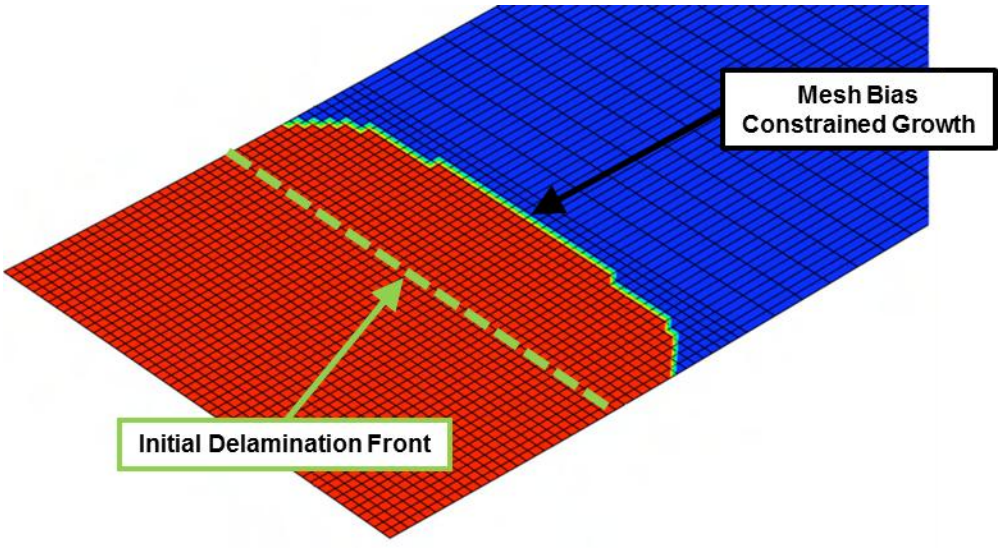

Figure 1. Jagged saw-tooth delamination growth via the nodal release method - resulting in mesh biased constrained growth. From [3].

initial delamination geometry is complex, and the growth pattern is unknown. Meshes should not provide a predetermined undue bias that obfuscates the physical results of a simulation.

This work proposes a new, general approach for the simulation of geometrically explicit delamination evolution. The geometry of the delamination front is continually updated and the finite element model is appropriately re-meshed around the updated front. This procedure of updating the delamination configuration and then re-meshing ensures the arbitrary nature of the evolution. The advance of the delamination and creation of new surface area are governed by a new energy-based formulation.

An incremental-iterative procedure utilizes the growth formulation to calculate point-wise advances along the delamination front. The geometry of the delamination drives the finite element simulation; the growth is not dictated by the finite element mesh, but by the mechanics and physics embedded within the energy-based growth formulation.

To use effectively the new energy-based growth formulation, fracture mechanics parameters must be accurately and efficiently calculated. A novel contribution of the new energy-based growth formulation is the use of the first order derivative of the energy release rate with respect to the delamination length, the rate of energy release rate, $\frac{dG}{da}$. The $\frac{dG}{da}$ parameter, in the 3-D sense, serves as an influence matrix that relates how an extension, da, at one point affects the energy release rate, dG, elsewhere along the front. The virtual crack extension (VCE)

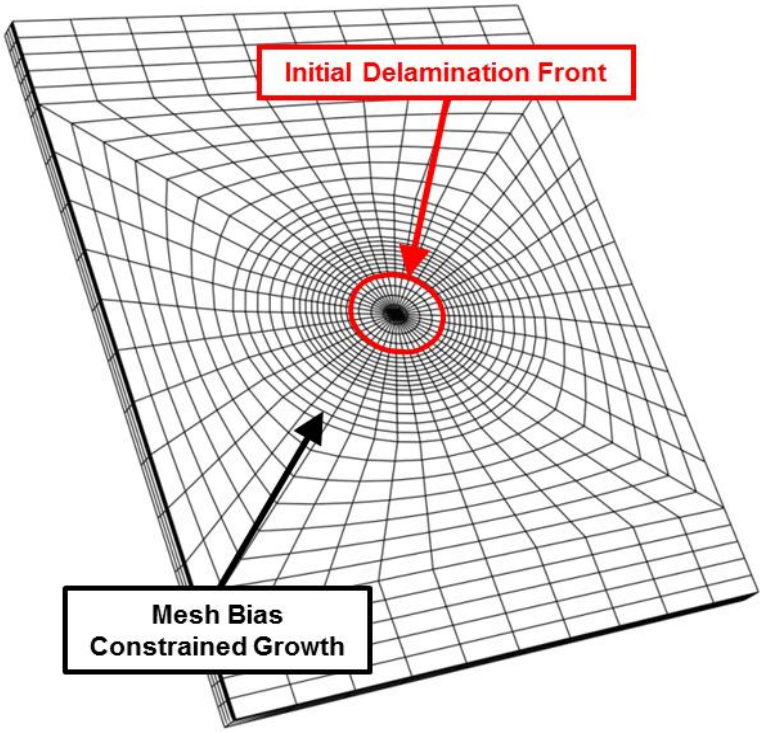

Figure 2. Pre-designed finite element mesh that adheres to expected growth pattern – resulting in mesh biased constrained growth.

method has been determined to be the most appropriate fracture mechanics tool, since it can extract both energy release rates and rates of energy release rate with a single finite element analysis. Other means of calculating the $\frac{dG}{da}$ parameter require a costly and time consuming finite difference approach. Another novelty presented is a VCE implementation that permits the decomposition of the energy fracture parameters, thus allowing the future use of mixed-mode fracture criteria.

The simulation technique incorporates three main components: 1) explicitly representing delaminations with re-meshing capabilities, 2) fracture calculations using the VCE method, and 3) prediction of growth using the new energy-based formulation. It should be noted that the techniques developed are independent. The energy-based growth formulation can be implemented using the VCCT (which has been done by the authors), or even be applied within the XFEM environment. The simulation methodology developed aims to achieve arbitrary delamination growth through representing the delamination as a geometric feature while reducing finite element bias.

The following sections will introduce the VCE method, providing background and a general framework. The implementation of the new 3-D, mixed-mode decoupling of energy release rates will be discussed. Verification results will be presented showing its effectiveness. The energy-based growth formulation will be introduced, describing the foundation and implementation of the method. Finally, the simulation of an embedded elliptical delamination subject to equal and opposite delamination face point loads is offered as a proof-of-concept for the new growth formulation.

THE VIRTUAL CRACK EXTENSION METHOD

The virtual crack extension (VCE) method, also known as the stiffness derivative method, is an energy approach first introduced by Dixon and Pook [6] and Watwood [7], and further developed by Hellen [8] and Parks [9]. Early VCE calculations utilized explicit perturbations of the finite element meshes to approximate the method's required stiffness derivatives. The finite difference approach of calculating derivatives often introduces geometric approximation and numerical truncation errors. Haber and Koh [10] developed a variational approach that eliminated the need for perturbations for stiffness derivative calculations. Lin and Abel [11] derived a similar method, rooted in variational principle theory, but generalized and simplified the required integration of [10]. Additionally, and importantly to the energy-based growth formulation herein, the approach of [11] permits the derivation of expressions for higher order derivatives of energy release rates. Hwang utilized the formulation of [11], generalizing the direct-integration approach for 2-D [12], multiply cracked bodies [13], and planar 3-D cracks [14]. The salient features of the VCE method are the accurate calculation of energy release rates and their derivatives, with a single finite element analysis.

Virtual Crack Extension Formulation

This section outlines the explicit expressions derived using the variational approach for the 3-D energy release rates and their derivatives. The following

formulation demonstrates the mathematical development of the VCE method. For a more complete mathematical derivation and discussion see [11] and [14].

The potential energy, Π, of a finite element system is given by

$$\Pi = \frac{1}{2}u^T K u - u^T f \tag{1}$$

where u, K, and f are the nodal displacement vector, the global stiffness matrix and the applied nodal force vector, respectively.

The energy release rate, G, at front position i is defined as the negative derivative of the potential energy with respect to an incremental front extension, da, at that position.

$$G_i \equiv -\frac{d\Pi}{da_i} = -\frac{1}{2}u^T \frac{dK}{da_i}u + u^T \frac{df}{da_i} \tag{2}$$

For simplicity, it is assumed that nodal forces are not influenced by the incremental virtual extensions. Therefore, the variational force term, $\frac{df}{da_i}$, goes to zero. The necessary parameters for a local energy release rate calculation at position i require nodal displacements and the variation in stiffness due to an incremental crack extension. The simplification reduces equation (2) to:

$$G_i = -\frac{1}{2}u^T \frac{dK}{da_i}u \tag{3}$$

It should be noted, however, if crack-face pressures, thermal, and/or body force loadings are considered, the variational force term must be included throughout the expressions and derivations.

The expression for the first order derivative of the energy release rate follows from the previous equations, by taking the variation of G_i in equation (3) with respect to another incremental crack extension, da, at position j.

$$\frac{dG_i}{da_j} = -u^T \frac{dK}{da_i}\frac{du}{da_j} - \frac{1}{2}u^T \frac{d^2K}{da_i da_j}u \tag{4}$$

The variation of displacements extends directly from the variation of the global finite element equilibrium equation, $Ku = f$, with respect to an incremental crack extension, da_j.

$$\frac{dK}{da_j}u + K\frac{du}{da_j} = \frac{df}{da_j} \tag{5}$$

Rearranging equation (5) and applying the simplifying assumption of $\frac{df}{da_j} = 0$, yields the expression for the variation of nodal displacements:

$$\frac{du}{da_j} = K^{-1}\left(-\frac{dK}{da_j}u\right) \tag{6}$$

The remaining derivations of the expressions for the stiffness derivatives can be found in [14]. These require a 'strain-like' matrix created by the virtual extensions applied to the front elements. The 'strains' are created by geometry changes of the finite elements in parametric space. Through the Jacobian and basis functions, variations in the strain-displacement matrices can be formulated, providing the components necessary for the stiffness derivative integrals.

Three-Dimensional Mixed-Mode Decomposition of Energy Release Rates

Several methods have been proposed to decompose energy release rates using the VCE method. [15] attempted to draw concepts used from the decomposition of the J-integral into J_1 and J_2. However, inaccuracies were discovered in the J_2 term when mode-II was dominant. [10] proposed a general 2-D method using Betti's reciprocal theorem and Yau's mutual energy representation. [11] used a similar approach that marries actual displacement fields with analytic solutions for pure mode-I and pure mode-II behavior. This is comparable to methods used in the interaction M-integral [16,17]. Ishikawa [18] developed a 2-D approach that first decomposed the displacements into mode-I and mode-II components using symmetry and skew-symmetry about the delamination front. The decomposed displacements were then used in standard VCE equations to calculate the mixed-mode energy release rates. This method was extended to 3-D by Nikishkov and Atluri [19] for the J-integral, and identified by [14] as a feasible 3-D approach for mode decomposition within the VCE method. One limitation to the symmetric/skew-symmetric technique is that a symmetric mesh is required around the front. This limitation is overcome through use of a front template that will be discussed later in the implementation section.

In the decomposition technique, displacement fields around a straight front can be separated into mode-I, II and III components. For an arbitrary front, the use of a local front coordinate system is required, Figure 3. A point-by-point coordinate transformation scheme is employed to essentially 'straighten' the front locally so the symmetric decomposition method can be used.

Once the front is in a local orientation, the mode-I, mode-II, and mode-III deformations can be decomposed with respect to the delamination plane along the local x_1 axis. Taking advantage of the symmetry of the finite element mesh

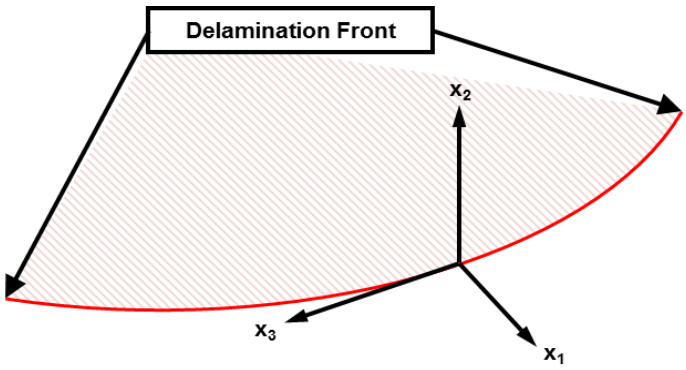

Figure 3. Local delamination front coordinate system.

surrounding the front, displacements u at point $P(x_1, x_2, x_3)$ and u' at $P'(x_1, -x_2, x_3)$, are used to decompose mode-I, mode-II and mode-III displacements at P.

$$u = u_I + u_{II} + u_{III} \tag{7}$$

$$u_I = \frac{1}{2}\begin{Bmatrix} u_1 + u_1' \\ u_2 - u_2' \\ u_3 + u_3' \end{Bmatrix} \tag{8}$$

$$u_{II} = \frac{1}{2}\begin{Bmatrix} u_1 - u_1' \\ u_2 + u_2' \\ 0 \end{Bmatrix} \tag{9}$$

$$u_{III} = \frac{1}{2}\begin{Bmatrix} 0 \\ 0 \\ u_3 - u_3' \end{Bmatrix} \tag{10}$$

With the displacements decomposed, and a transformed local stiffness derivative, denoted by the subscript ℓ, available, the following equation yields the mixed-mode energy release rates:

$$G_i = u_i^T \frac{dK}{da_\ell} u_i \text{ , where } i = I, II, III \tag{11}$$

Virtual Crack Extension Implementation

This section discusses the implementation of the VCE method, and the various numerical schemes employed to improve performance. The core of the VCE method has been implemented as a MATLAB post process. The MATLAB code reads in finite element information that identifies front nodes, elements, etc., and nodal displacements. The front is surrounded by a template comprising three rings of elements whose geometry can be carefully controlled. This satisfies the symmetric requirements of the mode decomposition method discussed previously and facilitates accurate fracture parameter calculations. The elements directly surrounding the front are either 20-noded brick or 15-noded wedge serendipity quarter-point elements, Figure 4.

The VCE procedure is applied across the front elements. Non-zero contributions to the stiffness derivatives occur only over elements involved with the virtual extensions. These elements are isolated for stiffness derivative calculations that are summed appropriately for a given virtual extension. Certain considerations must be addressed when dealing with a 3-D delamination. Along a 3-D front, virtual extensions between adjacent positions have an interaction component that must be accounted for in second order stiffness derivative calculations $\left(\frac{d^2K}{da_i da_j}\right)$. Also, the 3-D virtual extensions have an area associated with them depending on the element size that must be used to normalize the energy release rates and their derivatives. Since the formulation utilizes the variational approach, the virtual

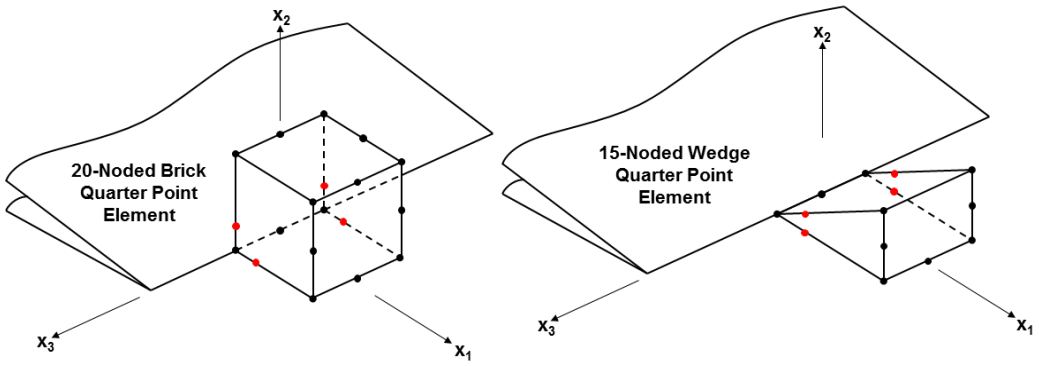

Figure 4. 20-noded brick and 15-noded wedge quarter point elements used to surround the delamination front.

extension applied can be of unit length; no optimized distance must be determined, thereby simplifying the implementation.

To ease the effort of computations, the use of an intermediate global force derivative parameter is employed. For each element involved with a particular front node i, first order stiffness derivatives are calculated then multiplied by the element nodal displacements.

$$dF_i = \frac{dK}{da_i} u \tag{12}$$

The force derivative parameter is mapped into a global environment and summed over the elements for the current front position. The global force derivative for each front node is stored in a matrix. This matrix is of size: number of degrees of freedom by number of front nodes, and is utilized in the calculation of the variation in displacements. Significant computational cost lies in the execution of equation (6). Unlike the stiffness derivative, the variation in displacements is a global calculation. The virtual extensions have an influence on all points within the finite element model. Equation (6) requires i-number of back solves with the symmetric global stiffness matrix and global force derivative. To accelerate the calculation and alleviate memory issues associated with the back solves, a standalone, parallelizable, sparse direct solver, MUMPS (**MU**ltifrontal **M**assively **P**arallel sparse direct **S**olver), is utilized.

VCE calculations can be conducted at corner or midside nodes along the front. The selection of corner or midside nodes alters the profile of the virtual extension: the former is linear, the latter quadratic. It was determined through a previous numerical investigation that calculations at corner nodes outperformed midside nodes. This observation agrees with results published in the literature for other methods [20].

Also incorporated in the implementation is the ability to carry out the numerical integration over one or two rings of elements, Figure 5. The single ring of integration comprises only quarter-point elements. The second ring utilizes the quarter-point elements and the next layer of surrounding brick elements. The theory behind adding the second ring is to improve results by effectively shifting

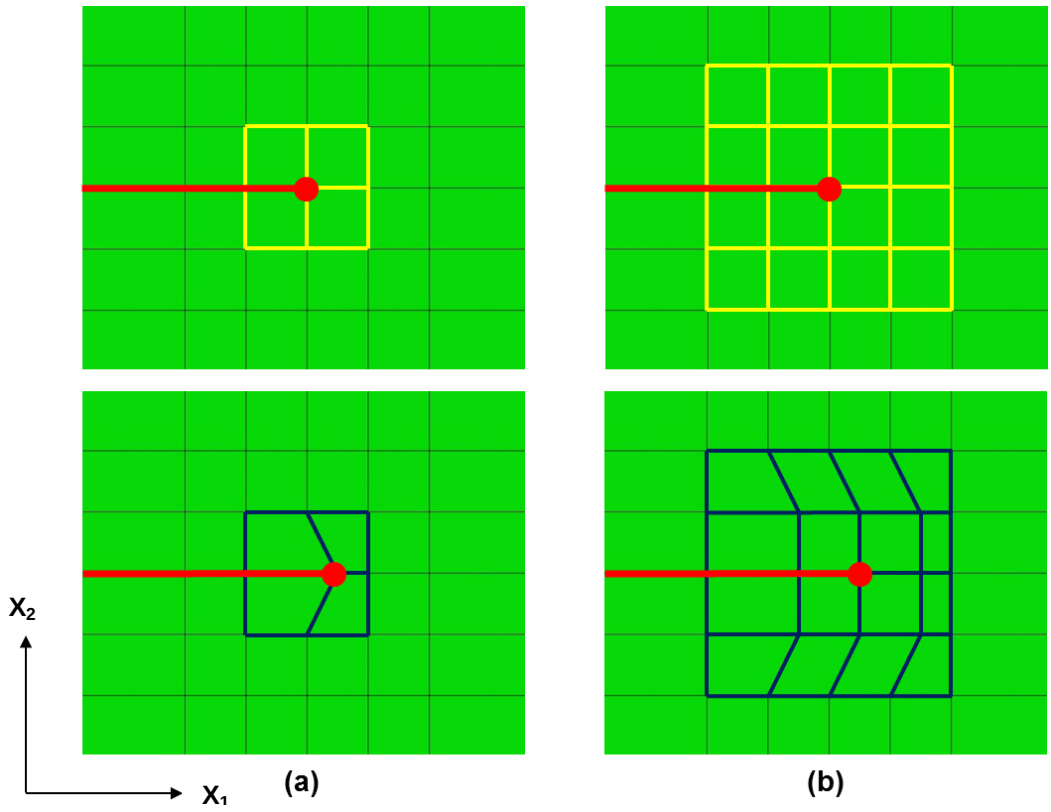

Figure 5. (a) 1-ring and (b) 2-ring elements involved in numerical integration for the VCE method. Top figures show the initial configuration. Bottom figures show the applied virtual extensions.

the area of high virtual strain caused by the virtual extensions away from the singular elements, to elements where field gradients are not as severe. The singular elements around the delamination front experience negligible virtual strain, i.e. shape and volume change in the element, and the brunt is moved to the second ring, Figure 6. In the same numerical investigation alluded to earlier, the second ring of integration was shown to provide more accurate results for both energy release rates and rates of energy release rate.

Herein, results will be reported only for the simplest, albeit still effective, form of the mixed-mode VCE method that uses quarter-point brick elements and a single ring of numerical integration at corner nodes along the front.

Verification Results for 3-D, Mixed-Mode Virtual Crack Extension Method

This section presents preliminary verification for the newly implemented 3-D, mixed-mode VCE method. To check the formulation and implementation, analytical displacements [22] from prescribed energy release rates were imposed on a straight front. Four scenarios were analyzed: 1) pure mode-I, 2) pure mode-II, 3) pure mode-III, and 4) mixed-mode I/II/III. In each instance an energy release rate of unity was prescribed.

For brevity, the results from the mixed-mode I/II/III scenario are shown in Figure 7. The pure mode-I, II, and III situations yielded similar levels of accuracy

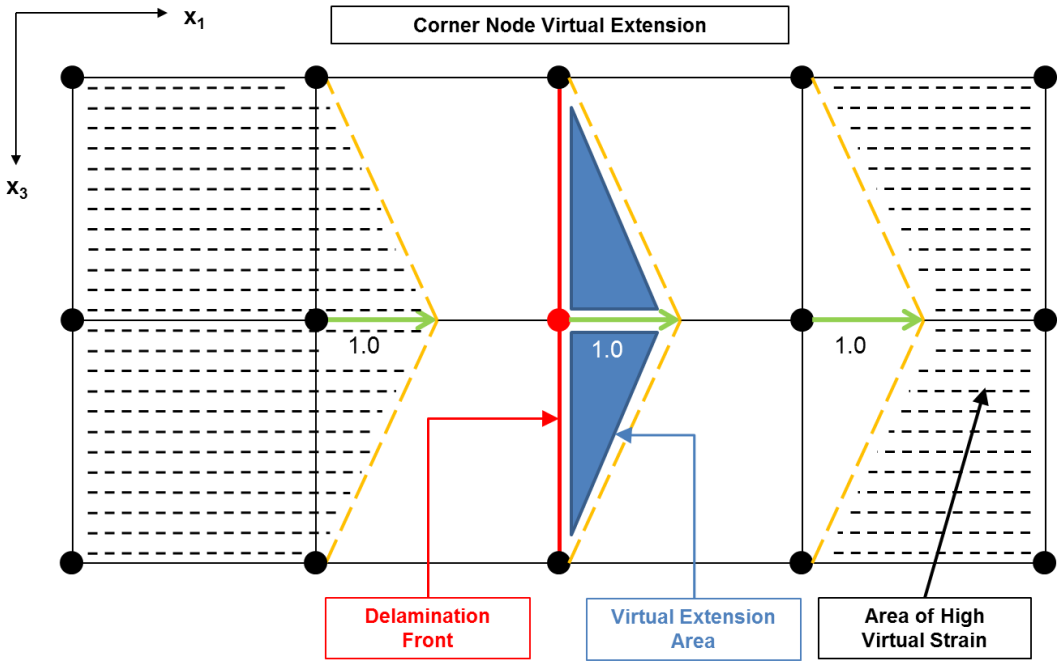

Figure 6. 2-ring virtual extension showing area of high virtual strain along the delamination front.

for their respective energy release rates. For each analysis, the decomposed energy release rates were within a fraction of one percent of the prescribed value. The energy release rates also agreed well with the total energy release rate calculations, verifying the known linear relationship.

ENERGY-BASED PREDICTION OF DELAMINATION GROWTH

The new energy-based growth formulation and implementation draw inspiration from experiences in plasticity. Both plasticity and delamination growth are characterized by behavioral transitions. These are denoted by a critical limit, for plasticity, the yield stress, and for delamination growth, a critical energy release rate. With this general connection between delamination growth and plasticity, a new formulation is developed for discretized front evolution.

Energy-Based Growth Formulation

The formulation extends directly from an expansion of the energy release rate.

$$G_{current} = G_{previous} + \frac{dG}{dP}\Delta P + \frac{dG}{da}\Delta a \tag{13}$$

The current energy release rate, $G_{current}$, is expanded into three components: the previous energy release rate prior to the load increment ΔP, $G_{previous}$, a portion due to the change in loading, $\frac{dG}{dP}\Delta P$, and a portion due to extension, $\frac{dG}{da}\Delta a$. Here $\frac{dG}{dP}$

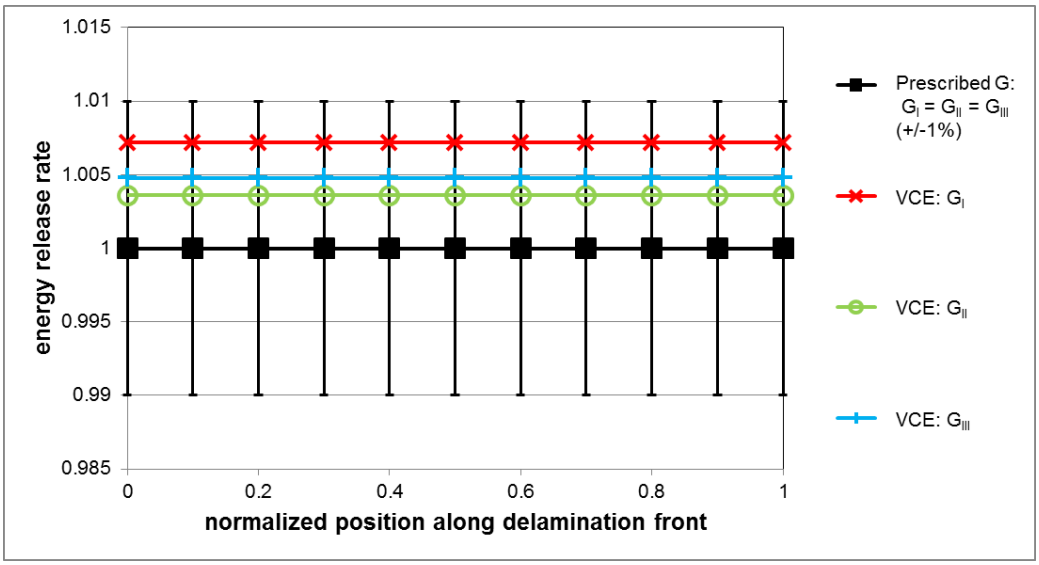

Figure 7. Mixed-mode energy release rate results using the 3-D VCE decomposition method.

characterizes the change in energy release rate with respect to the loading, $\frac{dG}{da}$ is the aforementioned influence matrix, and Δa is the extension increment. The expanded energy release rate forms a general stability equation that can be manipulated to calculate growth increments for an arbitrary front for a given load change.

A local front failure criterion must be selected. For simplicity, a local critical energy release rate, G_c, is set as the failure criterion. However, the formulation is not limited to this form of criterion. Effective energy release rates comprised of decomposed modes subject to power laws, etc. can easily be used with the formulation.

Two primary assumptions constrain the growth formulation to make results physically meaningful. The first asserts that the front cannot retreat, equation (14). The second restricts the current energy release rate from exceeding the critical criterion value, equation (15). Physically, the current front cannot exist at energy levels above the material's critical value, thus indicating a necessary change – i.e. the shape of the front.

$$\Delta a \geq 0 \tag{14}$$

$$G_{current} \leq G_c \tag{15}$$

Substituting the local failure criterion, $G_{current} = G_c$, into the general stability equation (13), yields the general growth condition.

$$G_c = G_{previous} + \frac{dG}{dP}\Delta P + \frac{dG}{da}\Delta a \tag{16}$$

This stability equation can be incorporated into an incremental loading scheme where resulting front extensions are calculated, determining a stable shape for each load increment.

Energy-Based Growth Implementation

The energy-based growth formulation is imbedded within an incremental-iterative procedure. This procedure requires an initially stable configuration. The delamination is then incrementally loaded. For each load increment, a growth condition is checked. If growth is detected, an iterative approach is employed using the energy-based growth formulation to achieve a stable configuration for that given load increment. If growth is not detected, the algorithm is allowed to proceed to the next load increment and continue on in the simulation. Figure 8 depicts the iterative scheme of the simulation technique that incorporates finite element model generation, analysis, fracture mechanics calculations, and the growth formulation.

As introduced previously, the mixed-mode virtual crack extension (VCE) method is used to calculate energy release rates along the front. Energy release rates need to be extracted for both the stable configuration, $\{G_{previous}\}$, and after the load increment, $\{G_{current}\}$. Here $\{\cdot\}$ denotes a vector of quantities, i.e. the energy release rate for each point along a discretized front.

At each load level, the VCE results are compared to critical values to determine if a growth condition is reached. The initial load level should be stable, meaning for all points along the front $\{G_{previous}\} < \{G_c\}$. After the load increment is applied, the energy release rates are checked again. Positions along the front are separated into mobilized, $\{G_{current}\}_m \geq \{G_c\}_m$, and stationary points, $\{G_{current}\}_s < \{G_c\}_s$. As the notation implies, the mobilized points are those that are expected to advance, where the stationary points, remain at their current locations. The mobilized points exceed the critical criterion for the given load increment, which is not physically attainable, indicating that an update in the front geometry is required.

The stability equation is rearranged and employed to determine the portion of the load increment, ΔP, that results in the mobilized positions going from stable

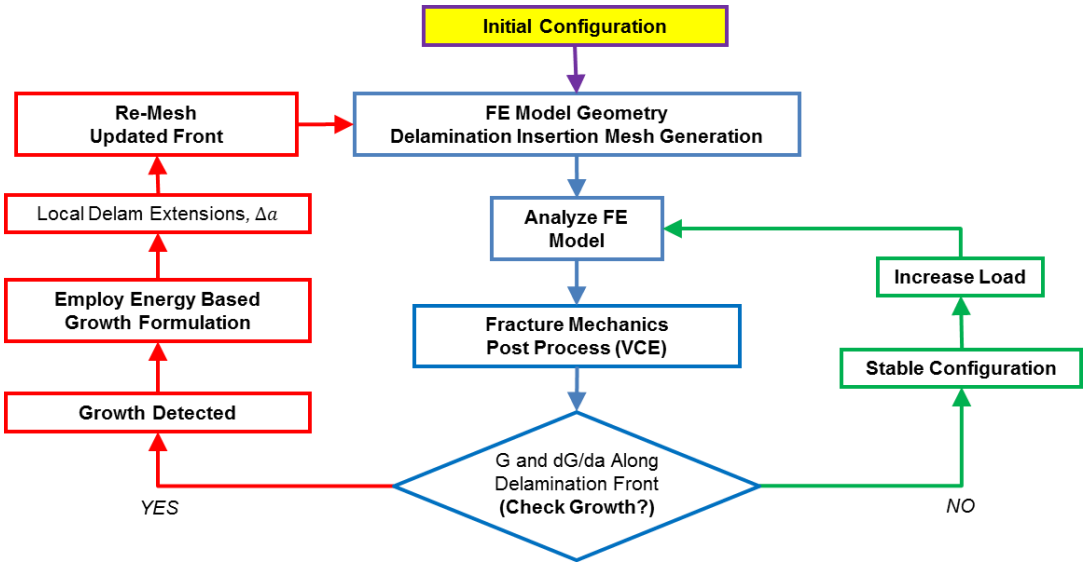

Figure 8. Simulation flow chart outlining use of finite element analysis, the VCE method, and the energy-based growth formulation in an iterative scheme.

$\{G_{previous}\}_m$ levels to the critical values, $\{G_c\}_m$. To determine ΔP_{crit}, it is assumed that the front geometry is unchanged, i.e. $\Delta a = 0$. Herein, the mobilized notation is dropped for clarity.

$$\{\Delta P_{crit}\} = \left\{\frac{dG}{dP}^{-1}\right\}\{G_c - G_{previous}\} \tag{17}$$

The $\left\{\frac{dG}{dP}\right\}$ term is obtained through a finite difference calculation between $\{G_{current}\}$ and $\{G_{previous}\}$. The ΔP_{crit} value for each of the mobilized positions along the front is subtracted from the total load increment, ΔP, to attain the portion of the load increment that contributes energy to the system resulting in extension.

$$\{\Delta P_{grow}\} = \{\Delta P\} - \{\Delta P_{crit}\} \tag{18}$$

In the next stage of the calculation, it is assumed that operations are centered at the local failure criterion. This sets $\{G_{current}\} = \{G_c\}$. The added energy $\{\Delta P_{grow}\}$ term is inserted back into the reorganized stability equation to calculate the delamination extensions for the mobilized positions, $\{\Delta a\}$.

$$\{G_c\} = \{G_{current}\} + \left\{\frac{dG}{dP}\right\}\{\Delta P_{grow}\} + \left[\frac{dG}{da}\right]\{\Delta a\} \tag{19}$$

$$\{G_c\} - \{G_{current}\} = 0 \tag{20}$$

$$\{\Delta a\} = -\left[\frac{dG}{da}\right]^{-1}\left\{\frac{dG}{dP}\right\}\{\Delta P_{grow}\} \tag{21}$$

The $[\cdot]$ notation signifies a matrix. Equation (21), with the use of the $\left[\frac{dG}{da}\right]$ influence matrix, makes this method unique and capable of capturing arbitrary delamination growth.

Each mobilized position along the front is advanced according to $\{\Delta a\}$ in an outward normal direction. The front geometry is updated, and re-meshed. With an updated finite element model, the iterative process is continued. The updated front geometry is loaded at the initial stable level prior to ΔP. A new $\{G_{previous}\}$ is calculated. The load increment is applied to the updated configuration. A new $\{G_{current}\}$ is calculated. A new set of mobilized and stationary nodes are identified. The previously described procedure is repeated with the new mobilized nodes, calculating the next iteration of extensions. The iterations are continued until a stable configuration is reached for the given load increment. The stability of the front geometry is achieved when, for all positions along the front, the energy release rates are below the failure criterion.

SIMULATION AND RESULTS

To test the formulation and implementation of the energy-based growth formulation, a proof-of-concept simulation was designed. The finite element re-

meshing, front advances, and model generations were carried out by in-house software. The models generated were imported into the ABAQUS finite element software. ABAQUS served as both the finite element environment and solver. The virtual crack extension (VCE) method used the ABAQUS results to calculate the necessary fracture mechanics parameters. The energy-based growth formulation was then employed to calculate point-by-point extensions for a given load increment.

An initial, embedded elliptical delamination, aspect ratio 2:1, in an isotropic material subjected to centrally applied point loads to the surfaces was simulated, Figure 9. Simple supports were used to prevent rigid body motion. For this example, a constant local critical energy release rate was chosen as the failure criterion. This configuration was selected because of its inherently stable growth. The elliptical geometry offers an opportunity to view non-uniform growth, rather than simulating a circular delamination that grows concentrically.

The load was separated into 25 increments. A stable configuration was reached for each load increment. On average, each increment required four iterations. The initially elliptical delamination evolved along the minor axis, eventually bowing into a circular configuration. Figures 10-15 show a sample of the stable configurations for selected load increments.

To assess the quantitative accuracy of the energy-based growth formulation, the simulation was continued to observe the circular growth pattern (Figures 14-15). Five concentric circular growth increments were simulated. An average percent difference of 0.1% was found for the simulated radii when compared to an analytical expression [21].

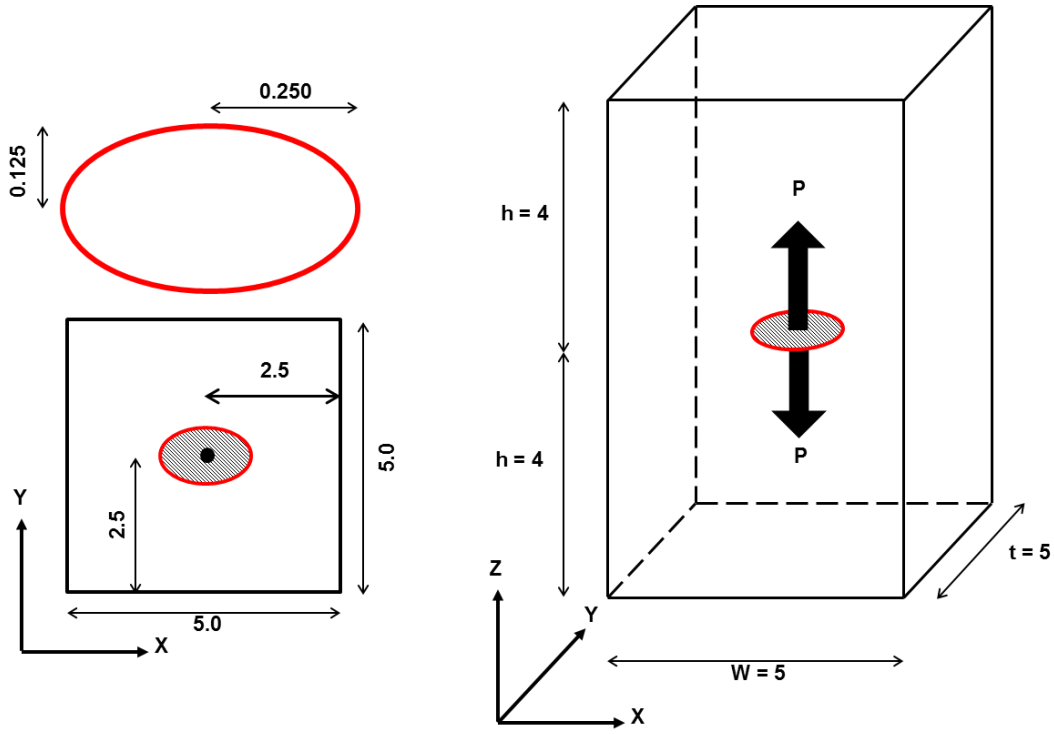

Figure 9. Geometry and boundary conditions for proof-of-concept simulation.

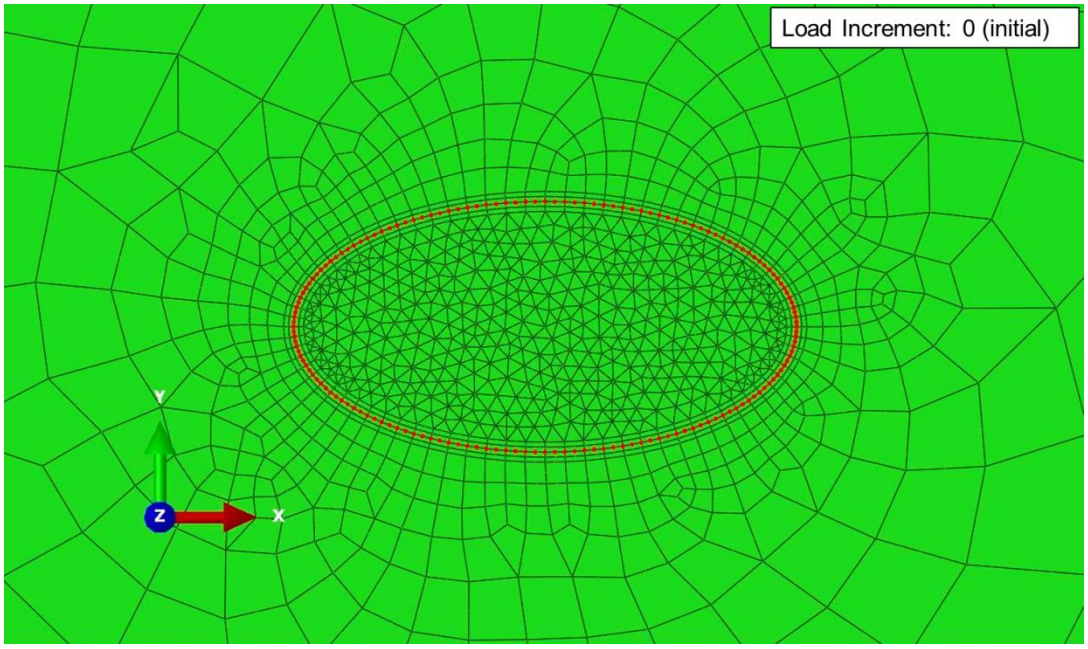

Figure 10. Simulation load increment 0 - initial elliptical delamination configuration.

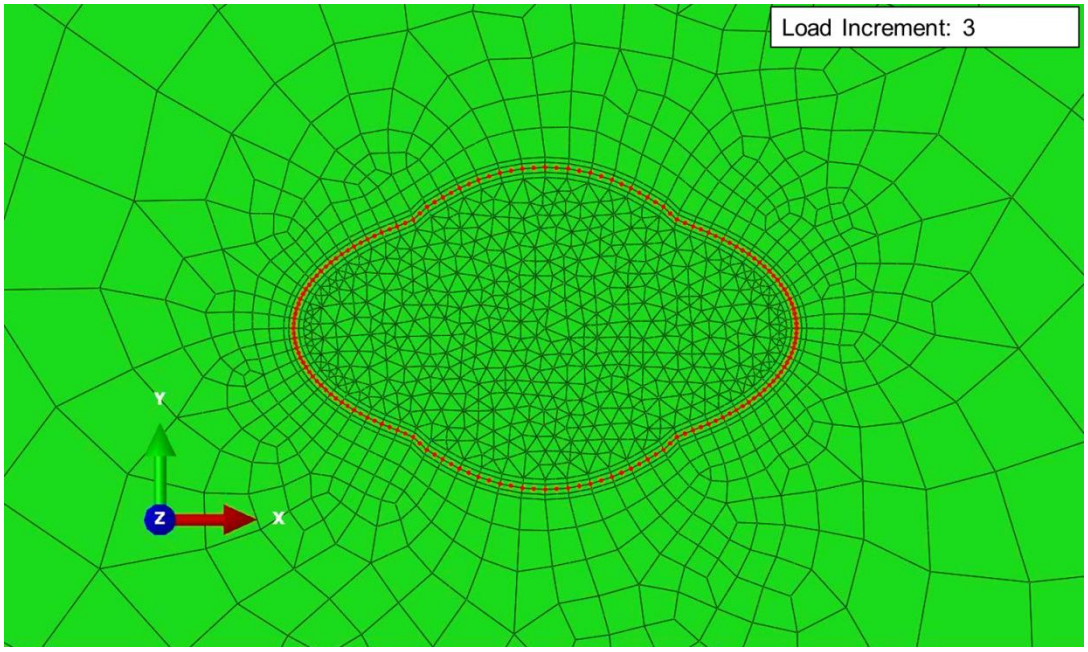

Figure 11. Simulation load increment 3.

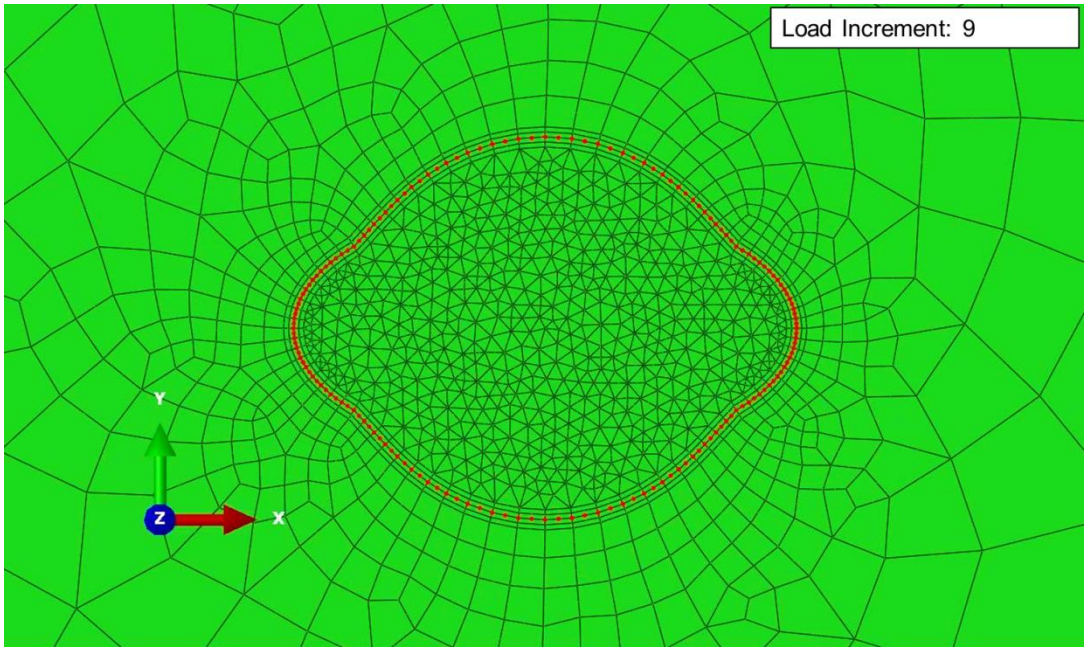

Figure 12. Simulation load increment 9.

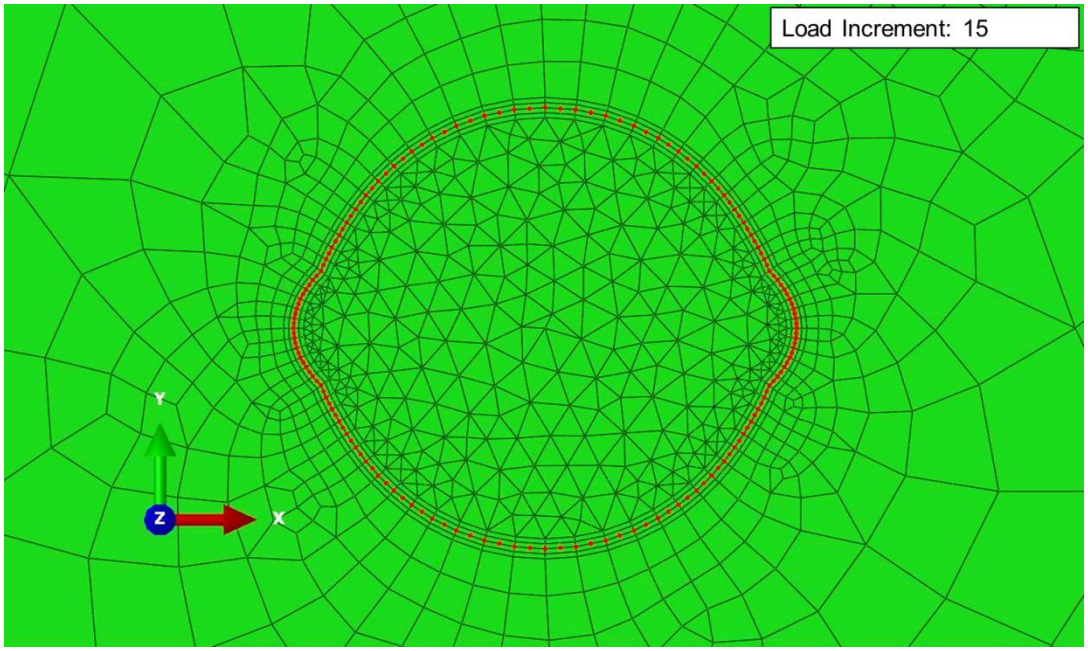

Figure 13. Simulation load increment 15.

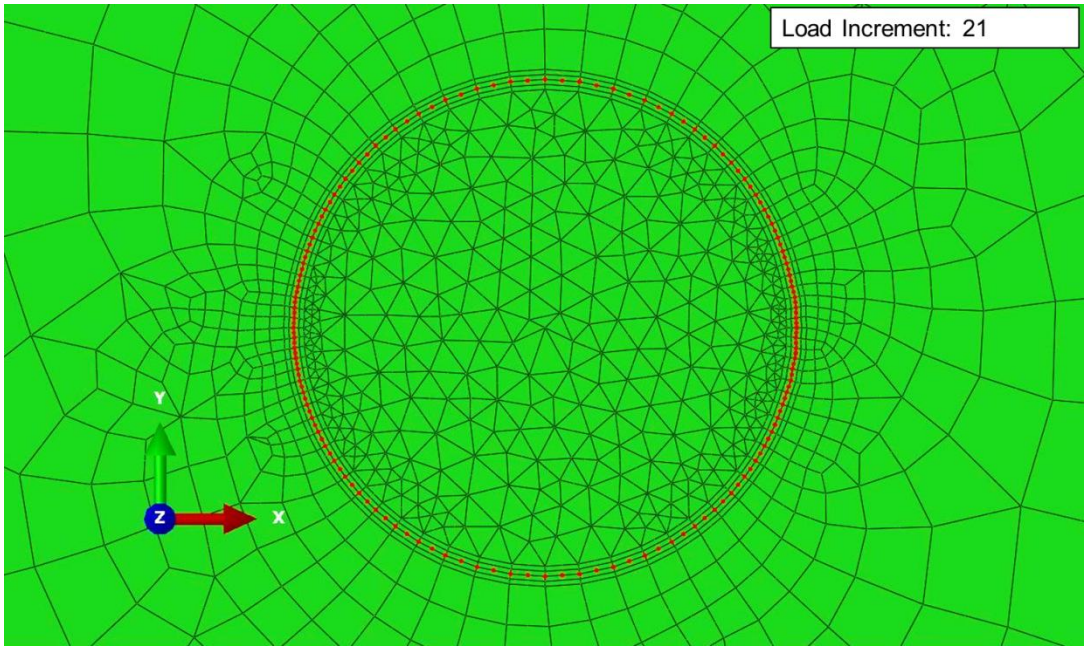

Figure 14. Simulation load increment 21.

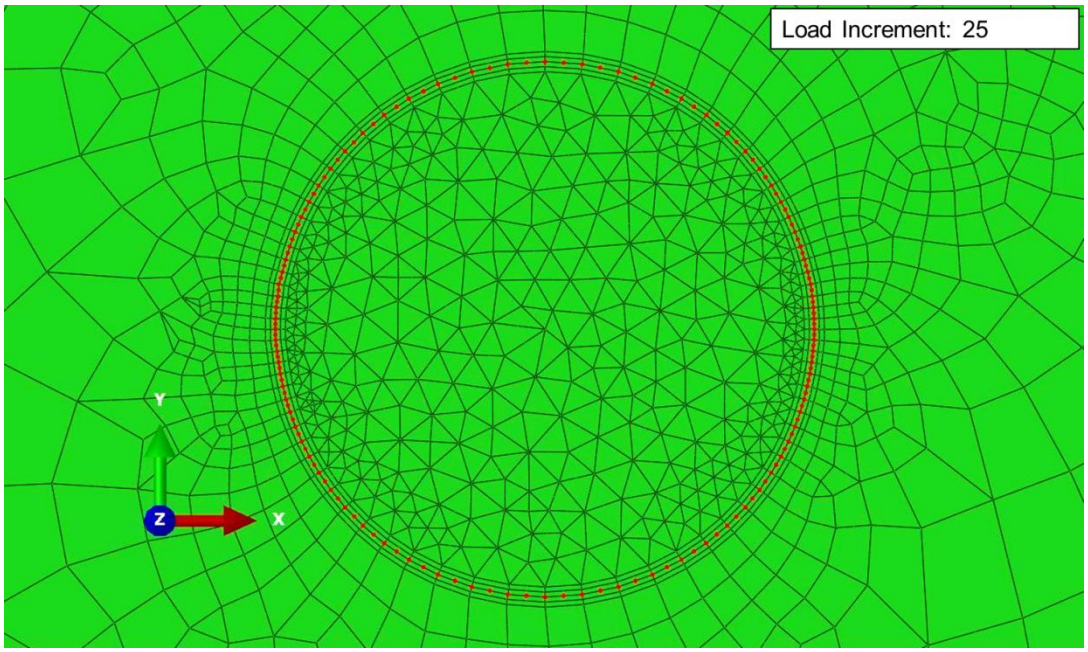

Figure 15. Simulation load increment 25 - final circular delamination configuration.

DISCUSSION AND CONCLUSIONS

The simulation technique, pairing the virtual crack extension (VCE) method and the energy-based growth formulation, has promise, as evidenced by the success of the proof-of-concept simulation. The VCE method offers an efficient and accurate means to calculate decomposed energy release rates and their derivatives. The energy-based growth formulation and its use of energy release rate derivatives, combined with re-meshing techniques, offer a general approach to the prediction of arbitrary delamination growth.

In previous work, the energy-based growth formulation was implemented using a finite difference approach with the virtual crack closure technique to calculate the $\left[\frac{dG}{da}\right]$ influence matrix. Each delamination front point was explicitly advanced, requiring a finite element calculation for each perturbed configuration. The energy release rate results from the perturbed fronts were then subtracted from the initial unperturbed front. This intensive process is cumbersome, requires a large number of iterations and is not as accurate. The VCE method improves both the accuracy of the influence matrix calculations and the overall shape predictions, which in turn reduce the number of iterations for each load increment.

When executing the energy-based growth formulation, there are two important considerations. The first requires a sufficiently discretized front. If too few points represent the front, each extension calculated and applied has a significant effect on the rest of the front. This could cause the iterative approach to become unstable. The second is the size of the load increment. To capture accurately the front evolution, the load step must be sized appropriately. If the load increment is too large, the algorithm might not reach a stable configuration.

The energy-based growth formulation does not rely on the configuration of the finite element mesh for its predictions of evolving fronts. The geometry of the front is the driving force of the simulation, and by smartly and effectively re-meshing around the front the accompanying computational cost is minimized. When dealing with finite elements, there are always influences associated with numerical approximations, e.g. discretized geometry, integration techniques. The energy-based growth formulation, however, reduces constraining bias from finite element meshes, allowing evolution of fronts to be driven by the physics.

This work presented the development and results of a novel, 3-D, mixed-mode VCE method implementation. It is attractive for use in composite delamination problems because of its energetic approach. The method requires only nodal displacements and stiffness variations, avoiding the use of oscillatory stress fields that exist at the delamination front between two different materials. Also introduced was a new energy-based growth formulation that makes use of the $\frac{dG}{da}$ term made readily available via the VCE method. The $\frac{dG}{da}$ term acts as an influence matrix, relating arbitrary growth along the delamination front. Since the growth formulation employs energy concepts, the methods are materially agnostic and can extend to problems concerned with non-linear material behavior. The approach to delamination growth simulation outlined in this work can be used to improve both design and in-life residual strength predictions, leading to more efficient use of material, optimal structural health monitoring, and more accurate overall life estimates.

AKNOWLEDGMENTS

The authors would like to thank the NASA University Institutes Project for their cooperation and financial support of the current work under Grant NCC3-989.

REFERENCES

1. Maimí, P., P.P. Camanho, J.A. Mayugo, C.G. Dávila. 2007. "A continuum damage model for composite laminates: Part I – Constitutive model," *Mechanics of Materials*, 39(10): 897-908.
2. Alfano, G., M.A. Crisfield. 2001. "Finite element interface models for the delamination analysis of laminated composites: mechanical and computational issues," *Int. J. Numer. Meth. Engng.*, 50(7): 1701-1736.
3. Krueger, R. 2008. "An Approach to Assess Delamination Propagation Simulation Capabilities in Commercial Finite Element Codes," NASA/TM-2008-215123.
4. Krueger R. 2004. "Virtual Crack closure technique: History, approach, and applications," *Appl. Mech. Rev.*, 57(2): 109-143.
5. Huynh, D.B.P., T. Belytschko. 2009. "The extended finite element method for fracture in composite materials," *Int. J. Numer. Meth. Engng.*, 77(2): 214-239.
6. Dixon, J.R., L.P. Pook. 1969. "Stress intensity Factors calculated generally by the Finite Element Technique," *Nature*, 224(5215): 166:167.
7. Watwood Jr., V.B. 1970. "The finite element method for prediction of crack behavior," *Nuclear Engineering and Design*, 11(2): 323-332.
8. Hellen, T.K. 1975. "On the method of virtual crack extensions," *Int. J. Numer. Meth. Engng.*, 9(1): 187:207.
9. Parks, D.M. 1974. "A stiffness derivative finite element technique for determination of crack tip stress intensity factors," *Int. J. of Fracture*, 10(4): 487:502.
10. Haber, R.B., H.M. Koh. 1985. "Explicit expressions for energy release rates using virtual crack extensions," *Int. J. Numer. Meth. Engng.*, 21(2): 301-315.
11. Lin, S., J.F. Abel. 1988. "Variational approach for a new direct-integration form of the virtual crack extension method," *Int. J. of Fracture*, 38(3): 217:235.
12. Hwang, C.G., P.A. Wawrzynek, A.K. Tayebi, A.R. Ingraffea. 1998. "On the virtual crack extension method for calculation of the rates of energy release rate," *Engng. Frac. Mech.*, 59(4): 521-542.
13. Hwang, C.G., P.A. Wawrzynek, A.R. Ingraffea. 2005. "On the calculation of derivatives of stress intensity factors for multiple cracks," *Engng. Frac. Mech.*, 72(8): 1171-1196.
14. Hwang, C.G., P.A. Wawrzynek, A.R. Ingraffea. 2001. "On the virtual crack extension method for calculating the derivatives of energy release rates for a 3D planar crack of arbitrary shape under mode-I loading," *Engng. Frac. Mech.*, 68(7): 925-947.
15. Hellen, T.K., W.S. Blackburn. 1975. "The calculation of stress intensity factors for combined tensile and shear loading," *Int. J. of Fracture*, 11(4): 605-617.
16. Banks-Sills, L., I. Hershkovitz, P.A. Wawrzynek, R. Eliasi, A.R. Ingraffea. 2005. "Methods for calculating stress intensity factors in anisotropic materials: Part I—z=0 is a symmetric plane," *Engng. Frac. Mech.*, 72(15): 2328-2358.
17. Banks-Sills, L., P.A. Wawrzynek, B. Carter, A.R. Ingraffea, I. Hershkovitz. 2007. "Methods for calculating stress intensity factors in anisotropic materials: Part II—Arbitrary geometry," *Engng. Frac. Mech.*, 74(8): 1293-1307.
18. Ishikawa, H. 1980. "A finite element analysis of stress intensity factors for combined tensile and shear loading by only a virtual crack extension," *Int. J. of Fracture*, 16(5): R243-R246.
19. Nikishkov, G.P., S.N. Atluri. 1987. "Calculation of fracture mechanics parameters for an arbitrary three-dimensional crack, by the 'equivalent domain integral' method," *Int. J. Numer. Meth. Engng.*, 24(9): 1801-1821.
20. Banks-Sills, L. 1991. "Application of the finite element method to linear elastic fracture mechanics," *Appl. Mech. Rev.*, 44(10): 447:461.
21. Sneddon, I.N. 1946. "The distribution of stress in the neighbourhood of a crack in an elastic solid," *Proc. Roy. Soc. London, Ser. A*, 187: 229-260.
22. Anderson, T.L. 2005. *Fracture Mechanics: Fundamentals and Applications*. Taylor & Francis Group, pp. 44-45.